

# Yields and Immunomodulatory Effects of Pneumococcal Membrane Vesicles Differ with the Bacterial Growth Phase

Mina Mehanny, Tobias Kroniger, Marcus Koch, Jessica Hoppstädter, Dörte Becher, Alexandra K. Kierner, Claus-Michael Lehr, and Gregor Fuhrmann\*

***Streptococcus pneumoniae* infections are a leading cause of death worldwide. Bacterial membrane vesicles (MVs) are promising vaccine candidates because of the antigenic components of their parent microorganisms. Pneumococcal MVs exhibit low toxicity towards several cell lines, but their clinical translation requires a high yield and strong immunogenic effects without compromising immune cell viability. MVs are isolated during either the stationary phase (24 h) or death phase (48 h), and their yields, immunogenicity and cytotoxicity in human primary macrophages and dendritic cells have been investigated. Death-phase vesicles showed higher yields than stationary-phase vesicles. Both vesicle types displayed acceptable compatibility with primary immune cells and several cell lines. Both vesicle types showed comparable uptake and enhanced release of the inflammatory cytokines, tumor necrosis factor and interleukin-6, from human primary immune cells. Proteomic analysis revealed similarities in vesicular immunogenic proteins such as pneumolysin, pneumococcal surface protein A, and IgA1 protease in both vesicle types, but stationary-phase MVs showed significantly lower autolysin levels than death-phase MVs. Although death-phase vesicles produced higher yields, they lacked superiority to stationary-phase vesicles as vaccine candidates owing to their similar antigenic protein cargo and comparable uptake into primary human immune cells.**

## 1. Introduction

*Streptococcus pneumoniae* is a bacterial pathogen that colonizes the upper respiratory tract and can invade other tissues leading to serious opportunistic diseases such as sepsis, meningitis and pneumonia. Approximately 1.5 million mortalities occur annually due to pneumococcal infections, especially in immunocompromised individuals, infants and older adults.<sup>[1–3]</sup> Thus, the World Health Organization considers *Streptococcus pneumoniae* a priority bacterium that requires urgent novel antibiotics or anti-infective strategies.<sup>[4]</sup> Pneumococci exhibit high genetic diversity owing to variation in the capsular polysaccharide structure, which is the main virulence determinant and dominant immunogenic structure. The introduction of the pneumococcal conjugate vaccine, which consists of a polysaccharide capsule conjugated to a carrier protein, induced a significant decline in invasive pneumococcal infections and a decrease in carrier and transmission cases.<sup>[5]</sup> However, the

M. Mehanny, G. Fuhrmann  
Helmholtz Institute for Pharmaceutical Research Saarland  
Biogenic Nanotherapeutics Group  
Campus E8.1, Saarbrücken 66123, Germany  
E-mail: gregor.fuhrmann@helmholtz-hips.de

M. Mehanny, C.-M. Lehr, G. Fuhrmann  
Department of Pharmacy  
Saarland University  
Campus E8.1, Saarbrücken 66123, Germany


M. Mehanny  
Department of Pharmaceutics and Industrial Pharmacy  
Faculty of Pharmacy  
Ain Shams University  
Cairo 11566, Egypt

T. Kroniger, D. Becher  
Center for Functional Genomics of Microbes  
Department of Microbial Proteomics  
Institute of Microbiology  
University Greifswald  
Greifswald 17489, Germany

M. Koch  
INM – Leibniz Institute for New Materials  
Campus D2.2, Saarbrücken 66123, Germany

J. Hoppstädter, A. K. Kierner  
Department of Pharmacy  
Pharmaceutical Biology  
Saarland University  
Saarbrücken 66123, Germany

C.-M. Lehr  
Helmholtz Institute for Pharmaceutical Research Saarland  
Drug Delivery Department  
Campus E8.1, Saarbrücken 66123, Germany

 The ORCID identification number(s) for the author(s) of this article can be found under <https://doi.org/10.1002/adhm.202101151>

© 2021 The Authors. Advanced Healthcare Materials published by Wiley-VCH GmbH. This is an open access article under the terms of the Creative Commons Attribution-NonCommercial-NoDerivs License, which permits use and distribution in any medium, provided the original work is properly cited, the use is non-commercial and no modifications or adaptations are made.

DOI: 10.1002/adhm.202101151

pneumococcal conjugate vaccine does not offer complete protection against all 100 known serotypes; it protects against only 13 serotypes. The pneumococcal polysaccharide vaccine (Pneumovax23) protects against 23 serotypes. Both vaccines face an increased prevalence of non-vaccine bacterial serotypes.<sup>[6–9]</sup> Therefore, researchers continue to seek additional, safe and effective vaccines against pneumococci.

Bacterial membrane vesicles (MVs) are lipid-bilayer structures with particle sizes ranging from 20 to 500 nm.<sup>[10,11]</sup> Previously, only gram-negative microorganisms were thought to release vesicles from their outer membrane and were thus called outer MVs (OMVs), whereas gram-positive bacteria were overlooked because their thick cell walls were considered to prevent vesicular secretion. However, over the last decade, many scholars isolated and tested MVs from gram-positive bacteria.<sup>[12]</sup> Gram-positive cell walls undergo local lysis and cytoplasmic membrane bulging, leading to bacterial vesicle and nanotube secretion.<sup>[13]</sup> MVs carry several cellular components that interact with the immune system, including immunogenic determinants and virulence factors; hence, they are being investigated in vaccine development.<sup>[14]</sup> MVs can interact with mammalian cells and successfully deliver their antigenic payload into immune cells. Consequently, they can induce considerable innate and adaptive protective immune responses against pathogenic bacteria in a safe and effective vaccine formulation.<sup>[11,15]</sup>

Nevertheless, bacterial MV production suffers from low and variable yields. Many factors influence the MV production process, yield and characteristics. Several studies devised methods to stimulate vesicular secretion, including application of sublethal antibiotic concentrations into bacterial cultures, a process that causes membrane perturbations and MV release. Gentamicin, polymyxin and colistin are among the most commonly used antibiotics.<sup>[16,17]</sup> Disturbing lipid-bilayer maintenance using bile salt sodium taurocholate is another technique to increase vesiculation.<sup>[18]</sup> Stress factors in the surrounding medium can enhance MV release, including altered oxygen tension and nutrient depletion.<sup>[19,20]</sup> Another technique is nitrogen cavitation to stimulate the generation of double-layered vesicles applied on *Pseudomonas aeruginosa* for vaccination purposes.<sup>[21]</sup> However, how such stress-induced MVs affect primary human immune cell viability and whether these MVs may be applied clinically remains unclear.

Application of bacterial MVs as vaccination avenues may suffer drawbacks including scarce and variable yields, low cellular uptake, unwanted cytotoxicity in primary human cells and weak protective immune responses. Therefore, we investigated how time of harvest during either, the stationary phase (24 h of bacterial growth) denoted stationary-phase membrane vesicles (sMVs) or death phase (48 h of bacterial growth) denoted death-phase membrane vesicles (dMVs), affects vesicular physicochemical properties. We assessed the effects, including enhanced yields of isolated vesicles, improved cellular uptake, altered proteomic pro-

files and potentiation of their immunostimulating effects, to generate bacterial MVs with promising vaccination potential.

## 2. Results and Discussion

Bacterial MVs are promising candidates as vaccination tools because they carry many microbial contents including lipopolysaccharides, cytosolic and membrane proteins, lipoproteins, and nucleic materials, which can interact with immune cells and initiate a protective immune response.<sup>[22]</sup> Pneumococcal MVs are considered miniature structures, with contents similar to those of their parent microorganisms.<sup>[11]</sup> We explored whether isolation during the death phase or the stationary phase, would affect vesicular yields, composition and immunogenicity to achieve better vaccine applicability.

### 2.1. dMVs Showed Higher Yields and a Slightly Higher Size Range to Those of sMVs

At 48 h, pneumococcal dMV yields were several folds higher ( $\approx 10^{12}$  particles mL<sup>-1</sup>) than the sMV yields, as determined via a nanoparticle-tracking assay. However, at 24 h, sMVs yielded  $\approx 10^{11}$  particles mL<sup>-1</sup> (Figure 1A). The yield was almost 10-fold higher, upon doubling the harvest time. We previously reported that fractions 6, 7, and 8 had the highest vesicle concentrations.<sup>[23]</sup> The dMVs exhibited a protein concentration of 404.33  $\mu\text{g mL}^{-1}$ , which is  $\approx 4 \times 10^{-10}$   $\mu\text{g}$  per vesicle, while the sMV protein concentration was 218.33  $\mu\text{g mL}^{-1}$ , which is  $\approx 2 \times 10^{-9}$   $\mu\text{g}$  per vesicle. We determined the vesicle concentration in terms of the number of particles per unit volume rather than the protein mass per fraction because proteins can originate from both vesicle membrane proteins and traces of nutrient medium as soluble protein impurities. Vesicular surface proteins, ligands, and/or antigens are biologically active, with suitable conformational structures and are located only on intact vesicles for relevant receptor binding. This is in contrast to soluble proteins, which can be ineffective or inactive.<sup>[24]</sup>

dMVs had a mean particle size of 150–200 nm, while sMVs ranged from 120 to 180 nm (Figure 1B). Size exclusion chromatography (SEC) enables adequately purifying vesicles while maintaining their biological activity, as we previously reported.<sup>[25]</sup> We successfully purified the resuspended pellet obtained after ultracentrifugation, as bicinichonic acid assay (BCA) confirmed adequate separation of MVs from soluble protein impurities. Visualizing dMVs via cryogenic transmission electron microscopy (cryo-TEM) enabled studying their morphology in detail (Figure 1C–H). Pneumococcal dMVs exhibited patterns similar to those of sMVs. Filtration allowed removing most of the protein impurities; thus, the pellet exhibited a clean background. Both vesicles showed very heterogeneous morphologies, with several arrangements and structures that included rounded, rod-shaped, irregular and chain-like vesicular forms. Additionally, some MVs showed darker contrast, suggesting different contents from those of other structures (Figure 1F). Many vesicles were detected within other vesicles; some smaller vesicles were budding from larger vesicles. Cryo-TEM investigation showed various particle sizes from 20 to 30 nm to  $\approx 200$  nm in diameter. Interestingly, some vesicles had double membranes, and others had

G. Fuhrmann  
Friedrich-Alexander-University Erlangen-Nürnberg  
Pharmaceutical Biology  
Department Biology  
Staudtstr. 5, Erlangen 91058, Germany

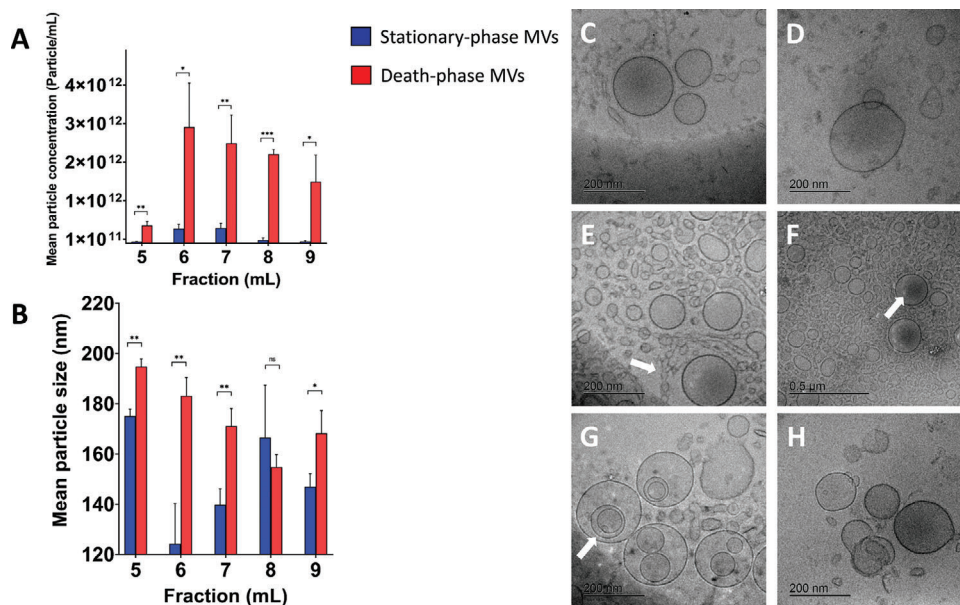


**Figure 1.** Nanoparticle tracking analysis results for stationary-phase membrane vesicles (sMVs) and death-phase membrane vesicles (dMVs). A) Average particle concentration of the collected size-exclusion chromatography vesicle-rich fractions, where all dMV-isolated fractions showed statistically significantly higher concentrations than did the sMV fractions as per unpaired two-tailed *t*-tests comparing individual fractions. B) Average particle size of collected vesicle-rich fractions, where most dMV fractions exhibited significantly increased particle sizes compared with those of sMVs as per unpaired two-tailed *t*-tests for individual fractions. The average number of independent experiments was  $n = 3$ , where each sample was recorded in triplicate; \* $p < 0.05$ , \*\* $p < 0.01$ , \*\*\* $p < 0.001$ , and *n*: non-significant (C–H). Cryogenic transmission electron microscopy investigation of isolated pneumococcal sMVs and dMVs. C, D) Isolated dMV pellet after ultracentrifugation; the white arrows show darker content structures E) and chain-like vesicle assembly F). Purified dMVs after size-exclusion chromatography, where the white arrows show superimposed G) and one-inside-another H) vesicle arrangement. Some vesicles were seen within each other (smaller vesicles were budding from larger vesicles). Particle size varied greatly, ranging from 20 to 30 to  $\approx 200$  nm in diameter.

darker contents, indicating that they may harbor different cargo than do other vesicular forms. Supporting Information Figures S3 and S4 show more cryo-TEM images of sMVs and dMVs.

Nanoparticle tracking analysis data showed a relatively larger particle size range for dMVs than sMVs, while both having a wide size range as determined by cryo-TEM images. The mechanism of vesicular biogenesis in gram-positive bacteria remains poorly understood; however, a complex global gene network is likely to be involved in MV production.<sup>[26]</sup> Heat-inactivated bacteria reportedly cannot produce MVs in their supernatants; only metabolically active microorganisms can undergo vesiculogenesis.<sup>[27]</sup> In both the stationary and death phases, viable and active bacterial cells can secrete their vesicles into the surrounding environment. This process starts with budding of the cytoplasmic membrane and depends on the turgor pressure of the membrane. Some lipidomic studies found similar fatty acid and phospholipid contents,<sup>[28]</sup> whereas other studies found differences in the phospholipid content between membrane vesicles and cell membranes.<sup>[29]</sup> dMVs showed significantly higher yields (i.e., more particles detected in the field), possibly because of collapsing cells or bubbling cell death via autolysin (Q7ZAK4);<sup>[12]</sup> our proteomic analysis data confirmed an abundance of autolysin in both vesicle types, especially in dMVs.

The higher yield might arise from increased MV release due to loss of membrane integrity or fragmented parts of the dying microorganism. Toyofuku et al. reported an increased release of MVs during lysis of *Bacillus subtilis*. Expression of prophage-

encoded endolysin in bacteria produced holes in the peptidoglycan wall, allowing MVs to protrude through it.<sup>[30]</sup> Nevertheless, a former study reported lower yield from dying pneumococcal cells, in contrast to our observation.<sup>[31]</sup> The bubbling mechanism from dying cells could explain the heterogeneous nature of pneumococcal vesicles isolated under both conditions, where dMVs are more abundant in terms of particle numbers. This is consistent with the findings of Resch et al. of heterogeneously sized circular structures, presumably for extracellular MVs from group A *Streptococci*.<sup>[27]</sup> Pneumolysin, a pore-forming toxin harbored on vesicles, can insert pores into lipid bilayers with protein-membrane aggregation of synthetic liposomes, causing membrane deformation and wrinkling and a layer-by-layer peeling of giant vesicles.<sup>[32]</sup> Pneumolysin (Q7ZAK5) was detected in our proteomic study of pneumococcal vesicles under both conditions. Therefore, pneumolysin may play a role in the heterogeneous morphology of pneumococcal vesicles.

## 2.2. Primary Human Immune Cells

### 2.2.1. Pneumococcal MVs Induced no Severe Cytotoxicity in Primary Human Immune Cells

To better understand the behavior and interactions of pneumococcal MVs inside the human body and confirm the suitability of applying bacterial vesicles for vaccinations, we examined the



## A Primary macrophages B Primary dendritic cells

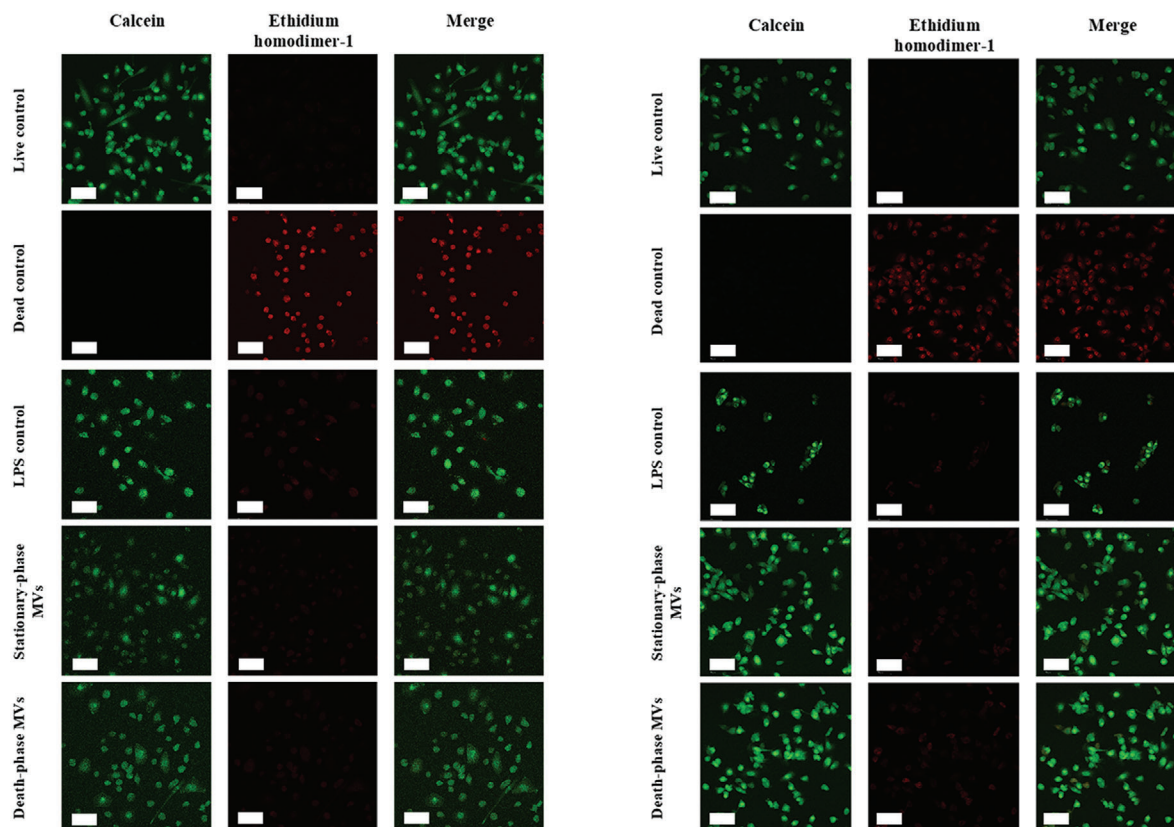


**Figure 2.** Confocal laser scanning microscopy images of primary human A) monocyte-derived macrophages (MDMs) and B) monocyte-derived dendritic cells (DCs) live-dead staining after treatment with stationary-phase membrane vesicles (sMVs) and death-phase membrane vesicles (dMVs) compared with live and dead controls and LPS-treated cells ( $250 \text{ ng mL}^{-1}$  for 8 h), where calcein (green) indicates live cells, and ethidium homodimer-1 (red) indicates dead cells (scale bar =  $50 \mu\text{m}$ )

compatibility with various epithelial and immune cells. We previously confirmed the excellent compatibility of pneumococcal MVs with cell lines as an initial indication of their safety,<sup>[23]</sup> thus, we assessed them with primary human immune cells to ensure their applicability for a safe and effective human vaccine.

Primary human blood-derived monocyte-derived macrophages (MDMs) and monocyte-derived dendritic cells (DCs) exhibited good viability upon incubation with pneumococcal vesicles for 8 h at concentrations reaching 5000 MVs per cell, showing minimal changes from the positive live controls (Figures 2 and 3 and Supporting Information Figure S5), whereas dMVs showed very faint reddish staining in the confocal images (Figure 2) due to the presence of few dead cells in MDMs and DCs. Concentrations up to 5000 vesicles per cell did not produce severe cytotoxicity and caused no major changes in cellular morphology or membrane integrity (Supporting Information Figure S6). Green fluorescence accumulated in the living cells, suggesting good tolerance with primary human cells, but further in vivo animal experiments are needed to confirm this finding. Both pneumococcal vesicles scored  $\approx 85\%$  viability with MDMs and  $75\%$  viability with DCs at a concentration of 5000 MVs per cell (Figure 3). No significant difference was

observed between pneumococcal MVs and LPS-treated immune cells.

However, some studies reported cytotoxic effects from other streptococcal strain vesicles. A study that isolated MVs from group B *Streptococci* showed hemolytic effects and induced cellular death of primary human cells after incubating neutrophils for 3 h and B and T cells for 1 h with  $10 \mu\text{L}$  of vesicles at  $2 \times 10^{-4} \mu\text{g}$  vesicle protein per cell using an LDH assay.<sup>[33]</sup> Group B streptococcal MVs disrupted the fetomaternal barrier in lab mice after intra-amniotic injection due to their matrix-degrading proteases and pore-forming toxins, causing preterm birth.<sup>[34]</sup> Our study showed acceptable compatibility and relative safety of pneumococcal vesicles, possibly owing to more efficient purification using SEC, and suggesting the vesicles' promising applicability for vaccines.

### 2.2.2. Pneumococcal MVs Showed Excellent Viability with cell Lines

Cellular viability was excellent upon treatment with several dMV and sMV concentrations for all examined cell lines, and no cytotoxic effects were observed (Supporting Information Figure S7).

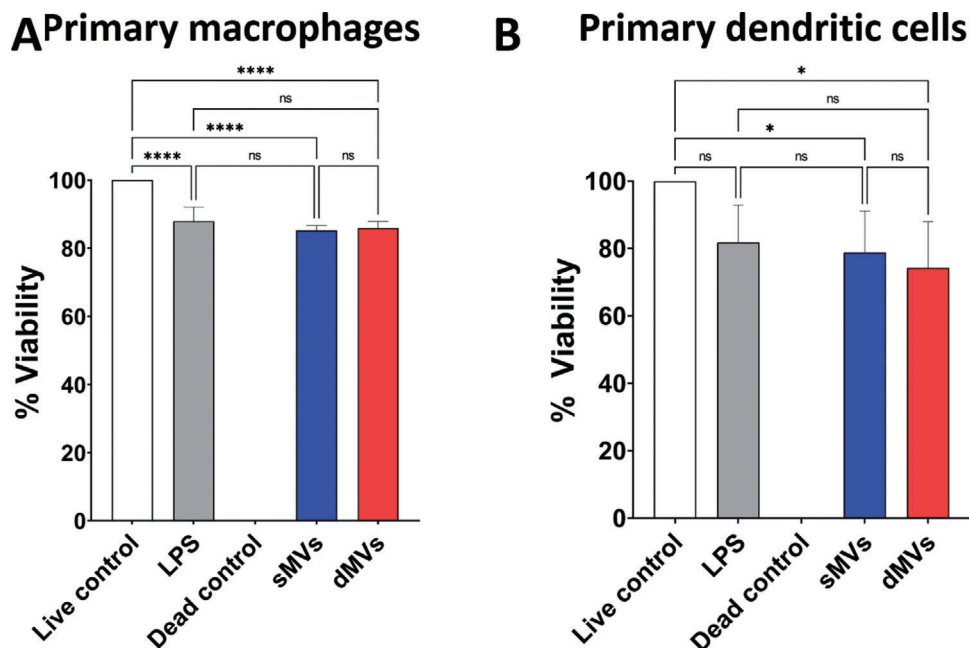


**Figure 3.** Quantitative determination of viability of primary monocyte-derived macrophages (MDMs) and monocyte-derived dendritic cells (DCs) via flow cytometry, using a live-dead kit. Cell viability percentage of stationary-phase membrane vesicles (sMVs) and death-phase membrane vesicles (dMVs) compared with live controls for A) MDMs and (B) DCs. Average number of independent samples ( $n = 4$ ), where each sample was recorded in duplicate, using cells from four donors. LPS treatment was at concentration of ( $250 \text{ ng mL}^{-1}$ ) for 8h. One-way ANOVA was applied, followed by a Tukey post-hoc test, where \*  $p \leq 0.05$ , \*\*\*\*  $p \leq 0.0001$  and ns = non-significant.

Epithelial cells, including pulmonary cells (A549) and skin cells (HaCaT), were used to assess the effects of dMVs and sMVs on these cells as potential routes for vaccine administration. The pulmonary route is an important infection pathway for pneumococci. Murine macrophages (RAW264.7) were used as examples of immune cells to test their potential safety for vaccination interactions. These cells were applied to confirm pneumococcal MV suitability before further primary human immune cell testing.

All cell lines showed very good tolerance to MVs upon 24 h incubation with concentrations reaching  $10^6$  MV per cell. Cellular viability even exceeded that of the positive live controls (PBS-treated cells with 100% calculated viability), as reported previously.<sup>[23]</sup> Higher vesicle concentrations yielded higher recorded viability values for A549 and HaCaT cell lines, while RAW264.7 cells demonstrated similar viability values for all applied vesicle concentrations. dMVs tended to have higher calculated viability than sMVs for A549 and HaCaT cells, while RAW264.7 cells demonstrated almost the same values for both vesicles, possibly due to consumption of these vesicles for cellular nutrition.<sup>[35]</sup> MVs might also stimulate the metabolic activity in the cells, leading to a stronger intracellular environment to reduce the resazurin PrestoBlue reagent to the fluorescent resorufin, leading to increased overall recorded fluorescence and hence, viability.<sup>[23]</sup>

Pneumococcal MVs caused negligible, if any, cytotoxic effects on all cell lines and at all concentrations applied. All cell lines tolerated high concentrations of pneumococcal vesicles up to  $10^6$  MVs per cell, without compromising their viability. RAW264.7 cells showed some cytotoxic effects at the highest concentration ( $10^6$  MV per cell), with  $\approx 10\%$ – $20\%$  cell cytotoxicity.

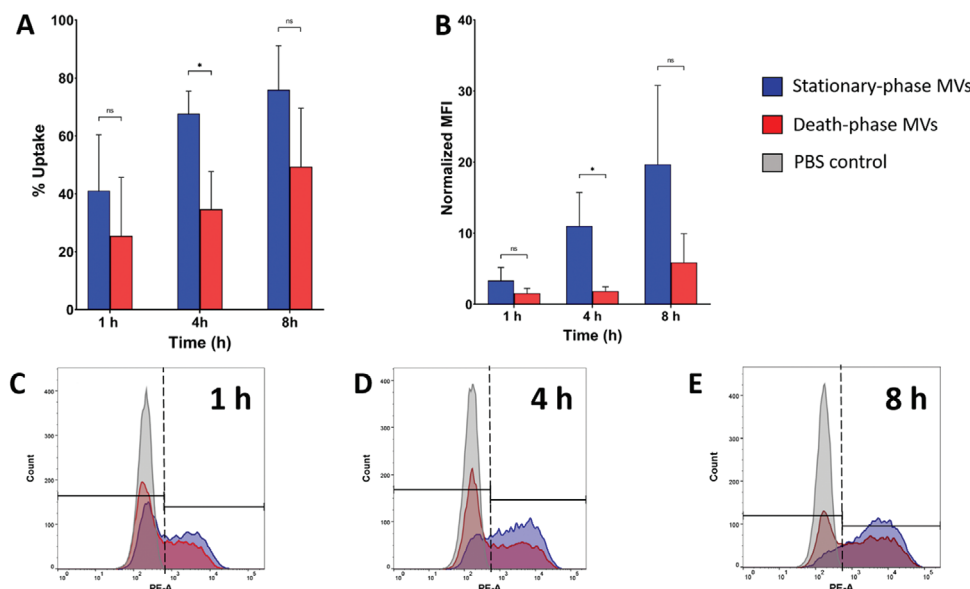
Consistent with our observations, a study reported that pneumococcal MVs lack cytotoxic effects on A549 cells for both sMVs and dMVs.<sup>[36]</sup> Codemo et al. similarly found that pneumococcal MVs could successfully internalize into A549 cells without causing cytotoxic effects after incubation for 24 h. These authors observed that pneumolysin-deficient mutant MVs produced no cell death in monocyte-derived DCs.<sup>[37]</sup> Although pneumolysin (Q7ZAK5) was identified in our vesicles, no cytotoxic effects were recorded in the cell lines or primary human immune cells.

### 2.2.3. Pneumococcal MVs were Taken Up Successfully by Primary Human Immune Cells

For successful vaccine development, vesicles should interact and colocalize and be successfully taken up by antigen-presenting cells. Therefore, we assessed the interaction and uptake of pneumococcal vesicles into primary human cells by analyzing DiI fluorescence-labelled vesicles via flow cytometry and confocal microscopy.

Both pneumococcal dMVs and sMVs showed gradual time-dependent uptake into primary human blood-derived MDMs and DCs. No significant difference in uptake into MDMs was observed except in 4h uptake samples, however sMVs displayed a slightly higher tendency to interact with human blood-derived primary MDMs than did dMVs at different time points, while both MVs exhibited similar uptake with DCs (Figure 4). Flow cytometry assays for uptake/interaction of fluorescent DiI-labelled vesicles into primary MDMs showed a fast interaction after 1 h of

## Primary macrophages



## Primary dendritic cells

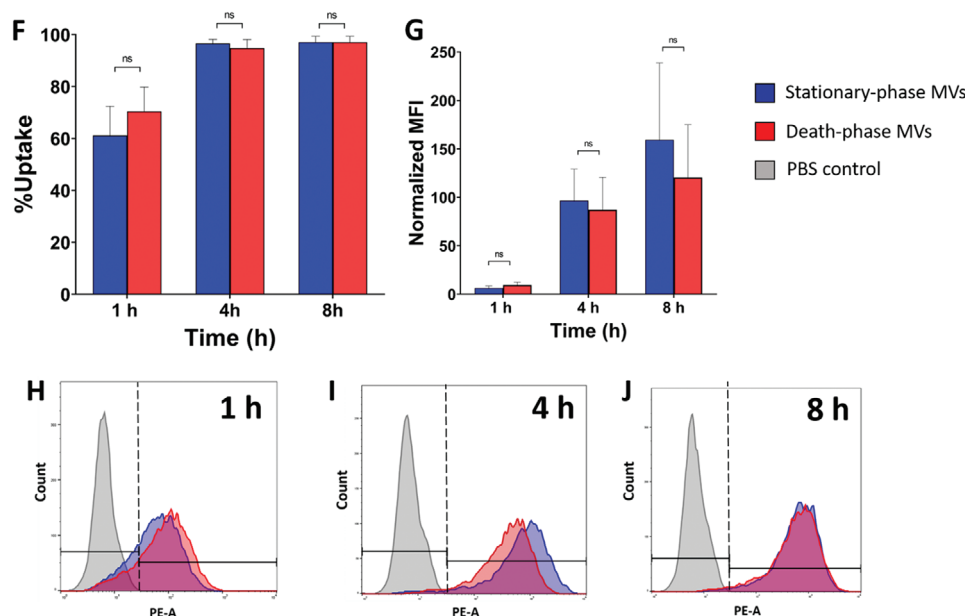


**Figure 4.** Uptake of DiI fluorescence-labelled stationary-phase membrane vesicles (sMVs) and death-phase membrane vesicles (dMVs) into human primary monocyte-derived macrophages (MDMs) and monocyte-derived dendritic cells (DCs) at 1, 4 and 8 h as per flow cytometry. Percentage uptake calculated as percentage of positive phycoerythrin (PE) cells at 1, 4 and 8 h compared with PBS-treated negative controls for MDMs (A) and DCs (F). Normalized median fluorescence intensity of MDMs (B) and DCs (G) after uptake of DiI fluorescence-labelled sMVs and dMVs compared with PBS-treated cells at 1, 4 and 8 h. Average number of independent experiments ( $n = 3$ ), where each sample was recorded in triplicate and compared using unpaired two-tailed t-tests between individual time intervals;  $^*p < 0.05$  and ns: non-significant (C–E and H–J) FlowJo analysis plots of PE-positive cells compared with PBS-treated cells at 1, 4 and 8 h, respectively. Average number of independent samples ( $n = 3$ ), where each sample was recorded in duplicate, using cells from four donors.

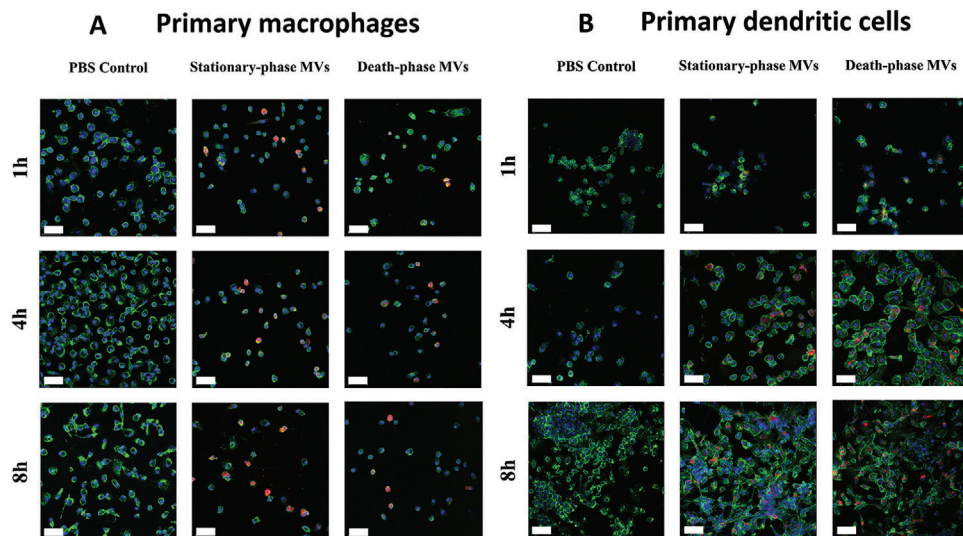


**Figure 5.** Confocal laser scanning microscopy of uptake of DiI (red) fluorescence-labelled stationary-phase membrane vesicles (sMVs) and death-phase membrane vesicles (dMVs) into human primary monocyte-derived macrophages (MDMs) at 1, 4 and 8 h (scale bar = 50  $\mu\text{m}$ ). Cell membrane glycoproteins were stained with fluorescein-wheat germ agglutinin (green) at 10  $\mu\text{g mL}^{-1}$  for 15 min, fixed in 3.7% w/v paraformaldehyde, and incubated with 1  $\mu\text{g mL}^{-1}$  DAPI (blue) for 15 min to stain the nuclei. Representative image for three independent experiments.

incubation of up to 40% for sMVs and 25% for dMVs. For sMVs, uptake reached 67% after 4 h and 75% after 8 h of incubation, whereas dMVs displayed 34% uptake after 4 h and 49% after 8 h of incubation. Faster uptake was recorded for primary DCs, reaching  $\approx 60\%$  and 70% after 1 h of uptake for sMVs and dMVs, respectively. Near complete uptake was achieved after 4 h of incubation for both vesicle types, supporting our previous observation that pneumococcal MVs are taken up rapidly by antigen-presenting DCs.<sup>[23]</sup>

Confocal laser scanning microscopy images showed successful internalization of pneumococcal vesicles into primary MDMs and DCs (Figure 5). After 1 h of incubation, minimal intracellular localization occurred in the cells because few red DiI-labelled MVs were observed within or attached to the green-stained cytoskeleton for both vesicle types. Internalization of vesicles inside macrophages increased gradually after 4 and 8 h, where sMVs exhibited slightly higher uptake than did dMVs. DCs demonstrated faster uptake, and nearly all cells internalized the vesicles after only 4 h of incubation. This supports the flow cytometry results that pneumococcal vesicles can successfully interact and colocalize inside immune cells and suggests successful delivery of loaded antigens for antigen presentation and immune response elicitation. Another study reported successful uptake of pneumococcal vesicles into monocyte-derived DCs after 2 h of incubation, supporting our results.<sup>[37]</sup>

In summary, both sMVs and dMVs demonstrated gradual time-dependent uptake into primary MDMs. Internalization of pneumococcal MVs into immune cells might play a role in antigenic payload delivery and interaction with cells to elicit an immune response. No statistically significant differences were observed, although sMVs tended to have higher uptake into cells than did dMVs. This suggests that some dMVs are merely bacterial cell fragments and might possess a vesicular structure or morphology but lack functionality or ability to traverse biological membranes.

#### 2.2.4. Pneumococcal MVs Stimulated the Release of Inflammatory Cytokines from Primary Human Immune Cells

We tested the ability of pneumococcal vesicles to stimulate primary MDMs and DCs to elicit a protective immune response for vaccination purposes. Measurement of released cytokines into the supernatant medium of primary MDMs and DCs upon 8-h incubation with pneumococcal MVs showed stimulated release of TNF and IL-6 (Figure 6). Both sMVs and dMVs exhibited similar effects on cytokine release, and no significant differences were observed. IL-8 could not be quantified because its concentrations exceeded the detection limit in both untreated and treated samples. However, four cytokines (IL-1 $\beta$ , IL-2, IL-12p70 and IFN- $\gamma$ ) were undetected in the collected supernatant, possibly because they are not secreted in large amounts from macrophages or only secreted after longer times.<sup>[38]</sup> IL-8 is a major chemokine that enhances neutrophil and monocyte migration to inflammation sites. Monocytes and macrophages secrete IL-6 upon stimulation of their pattern recognition receptors including toll-like receptors with pathogen-associated molecular patterns. IL-6 plays a crucial role in host defenses against infection and causes acute-phase response and fever.<sup>[39]</sup> TNF is necessary in protecting against pathogens and is produced from effector T cells and innate immune cells to initiate killing infected cells.<sup>[40]</sup> TNF and IL-6 levels were elevated upon treatment with pneumococcal vesicles, thus confirming the ability of pneumococcal MVs to initiate the inflammatory reaction necessary for a protective immune response. This indicates the potential of pneumococcal vesicles as vaccination tools.

#### 2.3. Proteomic Analysis of Isolated Pneumococcal MVs

In the MV proteomic analysis, we detected 586 proteins in isolated pneumococcal sMVs (24 h) and dMVs (48 h)



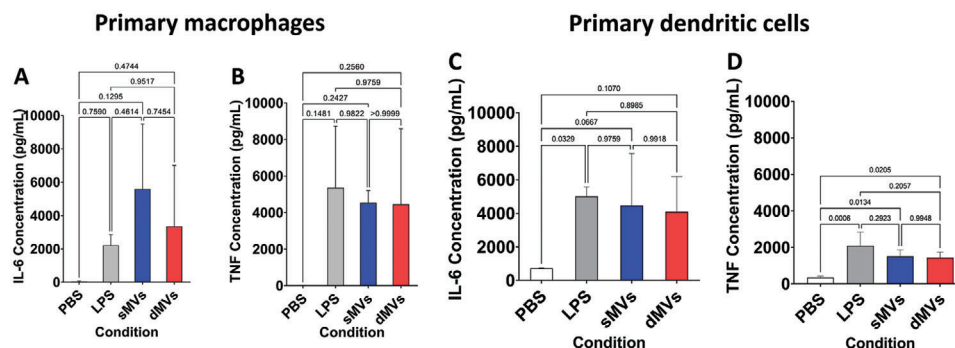


**Figure 6.** Determination of immunostimulatory cytokines released after incubation of pneumococcal stationary-phase membrane vesicles (sMVs) and death-phase membrane vesicles (dMVs) with human primary monocyte-derived macrophages (MDMs) and monocyte-derived dendritic cells (DCs) at concentration of 5000 MVs/cell, for 8 h compared with lipopolysaccharide (LPS)-treated controls at 250 ng mL<sup>-1</sup>. Concentrations of released interleukin-6 (IL-6) from MDMs (A) and DCs (C). Concentrations of released tumor necrosis factor (TNF) from MDMs (B) and DCs (D). Average number of independent samples ( $n = 4$ ), where each sample was recorded in triplicate, using cells from four donors. One-way ANOVA was applied, followed by the Tukey post-hoc test.  $p$ -Values are plotted between various samples.

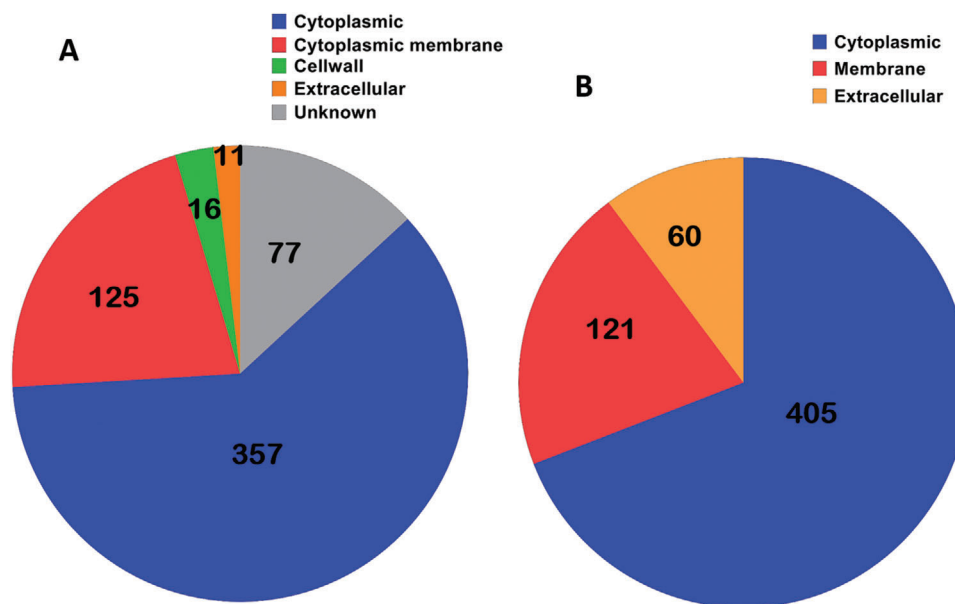


**Figure 7.** Subcellular localization prediction of shared proteins from the proteomic analysis in both pneumococcal stationary-phase membrane vesicles and death-phase membrane vesicles, using A) PSORTb and B) CELLO online databases.

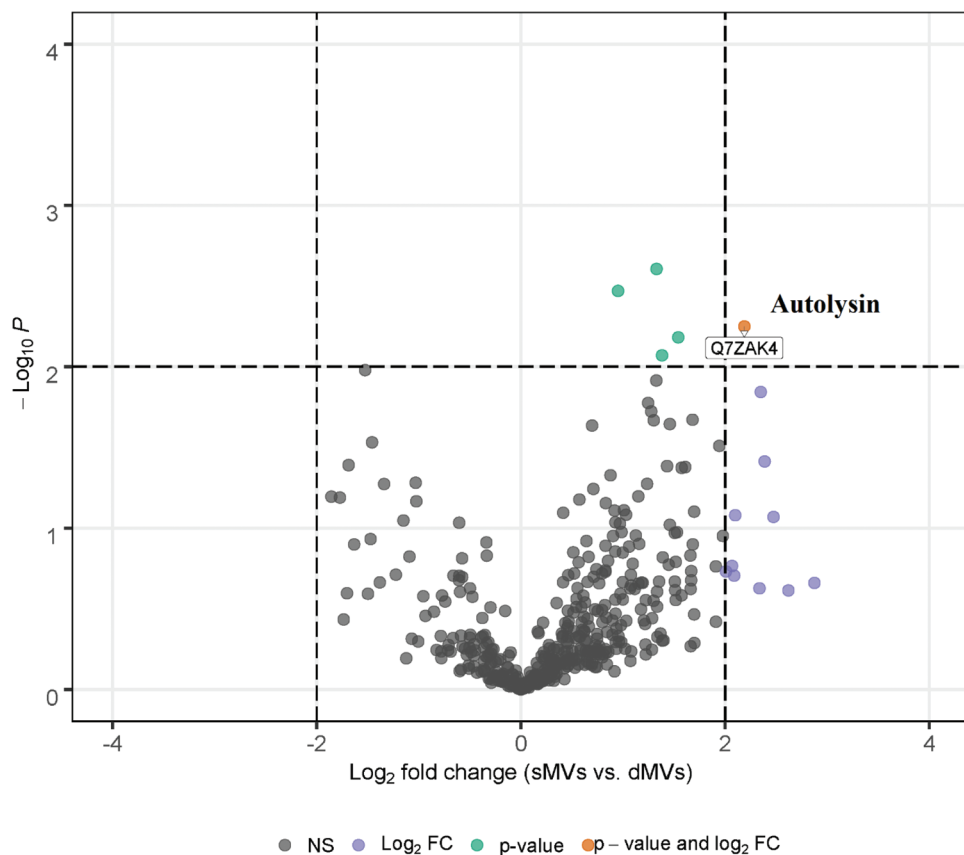
(Supporting Information File 1). We used the prediction tools, PSORTb and CELLO, to analyze the theoretical protein subcellular localization.

We used PSORTb, version 3.0.2 (<https://www.psorb.org/psorb/>), an online bacterial peptide subcellular localization prediction database hosted by the Brinkman laboratory, Simon Fraser University, British Columbia, Canada.<sup>[41,42]</sup> Most proteins in the sample (357 proteins) were assigned as cytoplasmic, followed by 125 cytoplasmic membrane proteins, thus showing a possible abundance of pneumococcal integral and transmembrane peptide proteins with probable antigenic characteristics. The program predicted that 16 proteins originated from the cell wall, and 11 were extracellular and might play roles as antigens and elicit an immune response. Seventy-seven proteins were considered to be of unknown origin (Figure 7A).

We applied another online tool, CELLO v.2.5, a subcellular localization prediction tool (<http://cello.life.nctu.edu.tw/>), ran by the Molecular Bioinformatics Center, National Chiao Tung University, Taiwan.<sup>[43]</sup> The platform predicted 405 proteins to be cytoplasmic, while 121 and 60 proteins were considered membrane and extracellular localized proteins, respectively (Supporting Information File 1; Figure 7B).

Autolysin (Q7ZAK4) was detected in both sMVs and dMVs. Interestingly, autolysin was significantly more abundant in the dMVs than in the sMVs (Figure 8). Autolysin is considered essential for pneumococcal virulence and for an immune response against pneumococci. Eleven proteins were detected exclusively in sMVs, and 30 proteins were exclusive to dMVs (Supporting Information File 1); none of these carried specific antigenic importance for vaccine development. Further, we studied how SEC





Total = 458 variables

**Figure 8.** Volcano plot of potential differences between measured proteins in both size-exclusion chromatography-purified stationary-phase membrane vesicles (sMVs) and death-phase membrane vesicles (dMVs). Significantly changed proteins are in orange ( $p < 0.01$ ,  $\log_2$  fold-change  $> 2$ ); proteins above the  $p$ -value threshold are in green; proteins above the fold-change threshold are in purple. The only significantly different protein between them was autolysin, which was significantly more abundant in dMVs. Supporting Information File 1 lists all identified proteins.

purification influenced both the sMV and dMV proteomes (Supporting Information Files 2 and 3). Only five proteins were found exclusively in the isolated sMV pellet, whereas many proteins were exclusive to SEC-purified sMVs (Supporting Information Figure S8). SEC-purified dMVs exhibited many exclusive proteins, whereas the pellet showed only sialidase A, as a single exclusive protein (Supporting Information Figure S9). The low number of exclusive proteins detected in the pellets after ultracentrifugation confirmed the robust nature of pneumococcal vesicles to ultracentrifugation and the absence of vesicular lysis during this process. Previous studies on pneumococcal vesicles reported that MVs are enriched with transmembrane proteins and lipoproteins.<sup>[31]</sup> Another study identified 61 putative antigenic proteins in pneumococcal vesicles, which might induce adaptive immunity.<sup>[36]</sup> Codemo et al. speculated that pneumococcal MVs are derived from the plasma membrane and carry some cytoplasmic proteins as well as surface proteins docked to the membrane.<sup>[37]</sup>

Proteomic analysis of pneumococcal MVs revealed additional information about their contents and potential functions (Supporting Information File 1). Several putative antigenic proteins and lipoproteins were abundant and identified in the isolated pneumococcal vesicles (Table 1). Pneumococcal

**Table 1.** Immunogenic proteins/lipoproteins detected in both stationary-phase and death-phase pneumococcal membrane vesicles during proteomic analysis.

Abundant immunogenic proteins/lipoproteins in pneumococcal vesicles	
<ul style="list-style-type: none"> <li>• Oligopeptide-binding protein (AliB)</li> <li>• Pneumococcal surface protein A (PspA)</li> <li>• Autolysin</li> <li>• Pneumolysin</li> <li>• Immunoglobulin A1 protease (IgA1 protease)</li> </ul>	<ul style="list-style-type: none"> <li>• Serine protease (PrtA)</li> <li>• Pneumococcal surface adhesin A (PsaA)</li> <li>• Choline-binding protein A</li> <li>• Pneumococcal histidine triad protein D</li> </ul>

lipoproteins play crucial roles for bacteria, including nutrient acquisition, resistance of stress conditions, enzymatic activities, and pathogenic processes such as adhesion, invasion and immune evasion. Additionally, lipoproteins trigger host innate immunity by activating toll-like receptor-2, which elicits strong cellular and humoral adaptive immune responses. Hence, lipoproteins are considered promising vaccine candidates.<sup>[44,45]</sup> Several lipoproteins were abundant in the analyzed MVs,

including phosphatidylglycerol-prolipoprotein diacylglycerol transferase (EC 2.5.1.145, Lgt) (Q8DPA3). Lgt is considered a crucial integral membrane enzyme involved in lipoprotein generation and its presence is essential for bacterial virulence and hence, immunostimulating effects.<sup>[46,47]</sup> Manganese ABC transporter substrate-binding lipoprotein (pneumococcal surface adhesin A, PsaA) (P0A4G3) was detected in both vesicle types, which is a surface lipoprotein abundant in all known pneumococcal serotypes and is responsible for manganese transport and acts as an adhesive for host cell attachment. PsaA was the third most abundant protein in our analysis. It is considered a strong virulence factor and highly immunogenic, leading to antibody formation against it, and is being evaluated for vaccine development.<sup>[48]</sup> In addition, other lipoproteins were present in both MVs including zinc-binding lipoprotein AdcA (Q8CWN2), lipoproteins (Q8DQ09) and (Q8DRG1) confirming their good immunogenic potential.

Pneumococcal vesicles harbored oligopeptide-binding protein (AliB) (P0A4G1), an ATP-binding cassette transporter involved in nutrient uptake and an important virulence factor that aids in nasopharyngeal colonization.<sup>[49]</sup> Autolysin (Q7ZAK4) is an important virulence factor and immunogenic protein loaded onto the vesicles, which causes the release of pneumococcal factors, inflammatory macrophage reactions and oxidative stress in pneumococcus-infected lung epithelial cells.<sup>[50,51]</sup> Pneumolysin (Q7ZAK5) is a key virulence determinant that induces pore formation, cellular damage, host tissue injury, and host immunity escape. It causes inflammatory responses and aids in transmission, colonization and cell death.<sup>[52]</sup> Importantly, it exhibits limited variation between different pneumococcal strains; thus, several studies have demonstrated its protective effect as an immunogenic agent.<sup>[53–55]</sup> Alkaline amylopullulanase (ApuA; Q8DRA6) is a cell-wall-anchored enzyme that hydrolyzes pullulan and glycogen in the nasopharyngeal and oral cavities, which might enhance mucosal adhesion and could be a virulence factor.<sup>[56]</sup> Another cell-wall-associated protein is serine protease (PrtA) (Q8DQP7), which is highly conserved among many pneumococcal strains. PrtA is a good candidate for vaccine development because it has strong immunogenicity, limited genetic variation and importance for pneumococcal virulence.<sup>[57,58]</sup> Another highly conserved pneumococcal protein is pneumococcal histidine triad protein D (Q8DQ08), which has been used in many studies of pneumococcal antigens for vaccination purposes. This protein induced functional antibodies and demonstrated a good safety profile and expanded protection against pneumococci in animal studies and clinical trials.<sup>[59–61]</sup>

Pneumococcal surface protein A (Q8DRI0) is a highly immunogenic protein, highly abundant on vesicles, and is a common vaccine candidate. It is expressed on the surface of all pneumococci, which confers promising potential for a protective immune response against pneumococcal infection.<sup>[62]</sup> It is reported to induce both systemic and mucosal immune responses, causing long-term T- and B-cell induction.<sup>[63–65]</sup> Immunoglobulin A1 protease (Q59947) is a proteolytic enzyme responsible for cleaving specific peptide bonds in the host's immunoglobulin A1 (IgA1) hinge region sequence. It is a crucial virulence factor in bacterial infection and colonization.<sup>[66]</sup> Monoclonal antibodies can inhibit its binding and block infection at the host interface.<sup>[67]</sup> Immunization using recombinant IgA1 protease

protected lab mice against lethal meningococcal and pneumococcal infections.<sup>[68]</sup> Choline-binding protein A (Q8DN05) is a member of a polypeptide family that anchors proteins to choline residues in the cell wall. It elicits the release of chemokines from activated endothelial cells and alveolar macrophages, leading to the recruitment of neutrophils into the alveolar space in early pneumonia.<sup>[69,70]</sup>

Olaya-Abril et al. performed lipidomic analysis of pneumococcal vesicles and confirmed that they are enriched in lipoproteins with slightly different fatty acid compositions from those of the bacterial cell membrane. Short-chain saturated fatty acids, especially lauric, myristic and palmitic acids, were enriched.<sup>[31]</sup>

These proteomic analysis data confirm the high potential of pneumococcal MVs as carriers for several highly immunogenic proteins and lipoproteins, which are considered promising multiple-antigen hybrid vaccine candidates against pneumococcal infections as a novel strategy for next-generation vaccines.<sup>[71,72]</sup> Our data indicate that dMV offer no advantage over sMV in terms of loaded antigenic proteins and lipoproteins, except for autolysin, which is significantly more abundant in dMV.

## 3. Experimental Section

### 3.1. Microbial Cultures and MV Isolation

We used *Streptococcus pneumoniae* reference strain R6 (American Type Culture Collection BAA255, VA, USA), which lacks a capsular polysaccharide, to maximize the isolated MV yield.

MVs were isolated as described previously.<sup>[23]</sup> Briefly, we grew bacteria for 24 h to isolate stationary-phase MVs (sMV) and 48 h to isolate death-phase MVs (dMV) in Bacto brain heart infusion nutrient medium (BD Biosciences) at 37 °C per 5% CO<sub>2</sub> (Supporting Information Figures S1 and S2). we collected the nutrient medium at 24 and 48 h, then centrifuged it twice at 3800 × g for 15 min at 4 °C to separate bacterial cells and unwanted debris. We filtered the supernatant using a Stericup Durapore PVDF 0.45 μm pore membrane filter (Merck Millipore, Darmstadt, Germany). Sterility was checked each time via overnight incubation under the same conditions to observe the absence of turbidity or changes in optical density at 600 nm. We added filtered supernatant into 70-mL ultracentrifuge polycarbonate tubes (38 × 120 mm, 355622, Beckmann Coulter, California, USA) and ultracentrifuged the tubes at 100 000 × g for 2 h at 4 °C using an SW 45Ti rotor (Optima L-90k, Beckman Coulter, California, USA). We removed the supernatant and resuspended the vesicle-rich pellet in 500 μL of filtered phosphate-buffered saline (PBS; Gibco PBS tablets lacking calcium, magnesium and phenol red; Sigma-Aldrich, Co., St. Louis, MO, USA) filtered through 0.2 μL cellulose ester filters (Whatman; GE Healthcare UK Limited, Little Chalfont, UK)

### 3.2. Purification

We transferred the resuspended pellet into a size-exclusion chromatography (SEC) column packed with Sepharose CL-2B (GE Life Science, UK) to remove soluble protein impurities and

obtain purified MVs. Eluted 1 mL fractions were collected in polypropylene tubes (Axygen, Corning Incorporated, Reynosa, Mexico).<sup>[35]</sup> The collected fractions were stored up to 2 weeks at 4 °C until used in further experiments.

### 3.3. Bicinchoninic Acid Assay

To purify and separate the MVs from the unwanted soluble protein impurities, we determined the protein concentrations from the collected SEC fractions using a bicinchoninic acid (BCA) assay kit (QuantiPro BCA Kit, Sigma Aldrich) per the manufacturer's recommendations. The samples were analyzed in triplicate using a calibration curve for standard bovine serum albumin.

### 3.4. Particle Size, Concentration and Size Distribution

We measured particle size distribution and MV yields via nanoparticle tracking analysis (LM-10, Malvern, UK). To achieve reproducible results, we diluted samples up to 1:1000 in filtered PBS to keep the MV concentration in the recommended range of 20–120 particles per frame. Briefly, 400  $\mu$ L of the diluted MV samples were introduced into a chamber illuminated by a green laser. Three 30 s high-sensitivity videos at a camera level of 13–15 were recorded and processed using Nanosight 3.1 software as previously described.<sup>[73]</sup>

### 3.5. Electron Microscopy

We performed cryogenic transmission electron microscopy (cryo-TEM) on MV pellets after ultracentrifugation and on purified SEC fractions as previously described.<sup>[23]</sup> Briefly, 3  $\mu$ L of the sample solution was dropped onto a carbon grid with holes (type S147-4, Plano, Wetzlar, Germany), then plotted for 2 s before plunging into liquid ethane at  $-165$  °C using a Gatan CP3 cryoplugger (Pleasanton, CA, USA). We transferred the sample under liquid nitrogen to a Gatan model 914 cryo-TEM sample holder and inspected it at  $-173$  °C via low-dose TEM bright-field imaging using a JEOL (Tokyo, Japan) JEM-2100 LaB<sub>6</sub> at 200 kV accelerating voltage. We acquired  $1024 \times 1024$  pixel images using a Gatan Orius SC1000 CCD camera with 4 s imaging time and binning 2.

### 3.6. Cell Cultures

We tested two human epithelial cell lines and one murine immune cell line. The human alveolar adenocarcinoma basal epithelial cell line, A549, was purchased from the German Collection of Microorganisms and Cell Cultures (DSMZ-ACC 107, Germany) and cultured in RPMI 1640 (Life Technologies Limited, Paisley, UK) supplemented with 10% (v/v) fetal calf serum (FCS). The human skin keratinocyte cell line, HaCaT, was obtained from Cell Lines Service GmbH (CLS-300493, Germany) and grown in Dulbecco's modified Eagle's medium (DMEM) supplemented with 10% (v/v) FCS. The murine macrophage

cell line, RAW264.7, was purchased from the European Collection of Authenticated Cell Cultures (Germany) and cultured in DMEM supplemented with 10% (v/v) FCS. A549, HaCaT and RAW264.7 cell lines were split once weekly, starting with  $0.2 \times 10^6$  cells/13 mL medium for A549 and RAW264.7 cells and  $0.4 \times 10^6$  cells per 13 mL medium for HaCaT cells. Mycoplasma tests were conducted regularly.

### 3.7. Viability of Mammalian Somatic and Immune Cell Lines upon Incubation with Pneumococcal Vesicles

To examine the mammalian cell viability upon treatment with several dilutions of pneumococcal MVs, cells were seeded into 96-well plates at 20 000 cells per well (A549 and RAW264.7) or 40 000 cells per well (HaCaT). All cell lines were cultured for 48 h until they reached 80%–90% confluence. During the assays, the medium was aspirated, and cells were cultured in fresh phenol red-free RPMI 1640 medium (Life Technologies Limited, Paisley, UK), not supplemented with FCS, to prevent any false results due to traces of lactate dehydrogenase (LDH) in the medium or extracellular vesicles in the serum. Cells were incubated with 100  $\mu$ L MV suspension in PBS at  $10^4$ – $10^6$  purified MVs per cell and 100  $\mu$ L of cell medium for 24 h. Live and dead controls were performed for each 96-well plate. A live control, in which cells were treated with PBS (100  $\mu$ L PBS added to 100  $\mu$ L medium), was run and showed no morphological changes. A dead control, in which cells were treated with 1% (v/v) Triton-X 100 (Sigma-Aldrich Co.), was run in parallel.

For the cytotoxicity assays, 100  $\mu$ L of medium was drawn from each well to perform an LDH assay, which measures the LDH released into the medium upon cell death and membrane disruption, and mixed with 100  $\mu$ L of LDH kit reagent (Roche Diagnostics GmbH, Mannheim, Germany) per the supplier's protocol. After incubating for 5 min at room temperature (RT), the absorbance was measured at 490 nm. For the viability assays, we used the PrestoBlue kit (Thermo Fisher Scientific, Waltham, MA, USA), which detects the metabolic activity in live cells, in a dilution of 1:10 with the respective cell culture medium. The remaining medium was aspirated, and 100  $\mu$ L of diluted PrestoBlue was added to each well, then incubated for 30 min at 37 °C. The dye fluorescence was determined at a 560 nm excitation wavelength and 590 nm emission wavelength using a Tecan Infinity Pro 200 plate reader (Tecan, Männedorf, Switzerland).<sup>[74]</sup>

### 3.8. In Vitro Isolation of Primary Human Monocyte-Derived Macrophages (MDMs) and Monocyte-Derived Dendritic Cells (DCs) from Buffy Coats

We isolated human monocytes from healthy adult blood donors (Blood Donation Center, Saarbrücken, Germany) and differentiated them using human macrophage colony-stimulating factor (M-CSF) (Miltenyi, 130-096-492) as reported previously.<sup>[75]</sup> Human material use and handling was reviewed and approved by the local Ethics Committees (permission no. 173/18; State Medical Board of Registration, Saarland, Germany). We isolated peripheral blood mononuclear cells (PBMCs) using density gradient centrifugation with Lymphocyte Separation Medium 1077

(Promocell, C-44010) and Leucosep tubes (Greiner Bio-One, 227290) per the supplier's recommendations. After washing with PBS, monocytes were separated from PBMCs by magnetic cell sorting using anti-CD14 microbeads (Miltenyi, 130-050-201) per the manufacturer's instructions, except that only 10% of the recommended bead amount was used as previously described.<sup>[76]</sup> Monocytes were seeded into 24-well plates ( $5 \times 10^5$  cells per well) and differentiated into macrophages in RPMI 1640 supplemented with 10% FCS, 1% (v/v) penicillin/streptomycin (100 units penicillin and  $0.01 \text{ mg mL}^{-1}$ ), 2 mM glutamine, and 20 ng  $\text{mL}^{-1}$  M-CSF at 37 °C and 5%  $\text{CO}_2$  for 6 days. DCs were differentiated using the same procedure and culture medium supplemented with interleukin-4 at  $10 \text{ ng mL}^{-1}$ .<sup>[77]</sup> The culture medium was changed on days 4 and 6, then further treated with vesicles on day 6.

### 3.9. Viability Assessment of Human Primary Human MDMs and DCs via Live-Dead Staining after Treatment with Pneumococcal MVs

Human primary MDMs and DCs were seeded at  $2 \times 10^5$  cells per well into 24-well plates in 500  $\mu\text{L}$  of the previously described medium. Cells were treated with pneumococcal vesicle suspensions (100  $\mu\text{L}$  per well) at  $5 \times 10^3$  vesicles per cell and incubated for 8 h. The MDM viability/cytotoxicity was measured using a Live/Dead staining kit (Invitrogen, ThermoFisher Scientific, L3224) via flow cytometry and confocal microscopy. In this assay, intracellular esterase activity in the live cells converts nonfluorescent cell-permeant calcein AM into intensely green-fluorescent calcein (excitation wavelength: 495 nm, emission wavelength: 515 nm). Ethidium homodimer-1 (EthD-1) accumulates in dead cells with damaged membranes by binding to their nucleic acids, producing a strong red fluorescence (excitation wavelength: 495 nm, emission wavelength: 635 nm); however, EthD-1 cannot permeate the intact plasma membranes of live cells. Cell viability/cytotoxicity was determined using flow cytometry per the manufacturer's recommendations. Briefly, cells were detached using Accutase solution (Sigma Aldrich, Germany, A6964) at 100  $\mu\text{L}$  per well at 37 °C for 30 min. Next, 2  $\mu\text{L}$  of 50  $\mu\text{M}$  calcein AM and 4  $\mu\text{L}$  of 2 mM EthD-1 were added to 1 mL of cell suspension ( $1 \times 10^6$  cells  $\text{mL}^{-1}$ ) and gently mixed. Afterwards, the cells were incubated for 15 min at RT in the dark, then analyzed using flow cytometry (LSR Fortessa, BD Bioscience, USA). Within each experimental set, we ran live and dead cell controls. Live controls were prepared using PBS (100  $\mu\text{L}$  per well), and these cells showed no changes in viability compared with that of medium-grown cells. Dead controls were prepared by heating the detached cell suspension in an 80 °C water bath for 10 min before conducting flow cytometry. LPS-treated cells were prepared at  $250 \text{ ng mL}^{-1}$  as controls. Stained cells were analyzed via flow cytometry at 488 nm of excitation and set to a 10 000 cell threshold. Cells were gated after excluding debris using two channels: Phycoerythrin-Texas Red-A (PE-Texas Red-A) for red fluorescence of EthD-1 within dead cells (610/20 bandpass) and fluorescein isothiocyanate-A (FITC-A) for green fluorescence of calcein within live cells (530/30 bandpass). Flow cytometry measurements were further analyzed using FlowJo 10.6.1 software (FlowJo LLC, USA). Cell viability/cytotoxicity was visualized us-

ing confocal microscopy per the manufacturer's manual. Briefly, 20  $\mu\text{L}$  of 2 mM EthD-1 was diluted in 10 mL sterile PBS and added to 5  $\mu\text{L}$  of 4 mM calcein AM, then vortexed thoroughly to achieve a working solution of 2  $\mu\text{M}$  calcein AM and 4  $\mu\text{M}$  EthD-1. Next, 150  $\mu\text{L}$  of working solution was added to the cells on glass slides and incubated for 45 min at RT. The cells were washed with PBS, and a drop of mounting medium (ThermoFisher, Germany) was added. The slides were then sealed with coverslips without damaging or shearing the cells. Images were captured using a Leica TCS SP8 confocal laser scanning microscope (CLSM, Leica Microsystems, Germany). Calcein was visualized using a 488 nm laser; EthD-1 was visualized using a 561 nm laser. Images were captured under a  $25 \times$  water-immersion objective lens at a  $1024 \times 1024$  resolution. Captured images were processed with LAS X software (LAS X 1.8.013370, Leica Microsystems).

### 3.10. Assessment of Uptake/Colocalization of Pneumococcal MVs within Primary Mammalian Immune Cells

After ultracentrifugation, the pelleted MVs were fluorescence-labelled via incubation with 2  $\mu\text{L}$  DiI (DiI Cell-labelling solution Vybrant, Thermo Fisher, Germany) for 30 min at 37 °C. Non-incorporated dyes were removed through an SEC column, and the fractions with the strongest fluorescence were further investigated.

Human primary blood-derived MDMs and DCs were seeded on 24-well plates ( $2 \times 10^5$  cells per well) and incubated for 6 days, then 100  $\mu\text{L}$  of labelled MVs were added at 5000 MVs per cell onto cells in 400  $\mu\text{L}$  of nutrient medium and incubated for 1, 4, and 8 h at 37 °C per 5%  $\text{CO}_2$ .

Cells were washed twice with PBS to discard any traces of labelled MVs, detached with 100  $\mu\text{L}$  per well Accutase solution (Sigma Aldrich, Germany, A6964) at 37 °C for 30 min, collected in 5 mL polystyrene round-bottom tubes ( $12 \times 75 \text{ mm}$  style, 352054, Falcon, Corning, USA) and diluted with 2% FCS in PBS until flow cytometry analysis (LSR Fortessa, BD Bioscience, USA).

### 3.11. Confocal Imaging of Cells for Uptake Study

Primary human blood-derived MDMs and DCs were seeded at  $2 \times 10^5$  cells per well on 8-well imaging slides (SPL Life Sciences, Korea), incubated for 6 days, treated with 100  $\mu\text{L}$  DiI-labelled MVs per well at the indicated concentration (5000 MVs per cell), and incubated for 1, 4, and 8 h. The supernatant was discarded, and cells were washed twice with sterile PBS, then incubated with fluorescein-wheat germ agglutinin (Vector Laboratories, USA) at  $10 \mu\text{g mL}^{-1}$  for 15 min at 37 °C per 5%  $\text{CO}_2$  to stain cell membrane glycoproteins.

Cells were then washed twice with PBS and fixed with 3.7% w/v paraformaldehyde for 20 min at RT. Nuclei were stained with 4',6-diamidino-2-phenylindole (DAPI) (Life Technologies, Germany) at  $1 \mu\text{g mL}^{-1}$  for 15 min at RT. The cells were washed, then a few drops of fluorescence mounting medium (Dako North America, USA) were added, and the slides were coverslipped.

Images were captured using a Leica TCS SP8 CLSM (Leica Microsystems), using a 488 nm laser to visualize fluorescein (green), a 405 nm laser to visualize DAPI (blue) and a 561 nm laser to visualize DiI (reddish-orange). We applied a  $25 \times$  water-immersion



objective lens with a minimum resolution of  $1024 \times 1024$  and speed of 200 for image capturing. Captured images were further processed using LAS X software (LAS X 1.8.013370, Leica Microsystems).

### 3.12. Determination of Released Cytokines from Human Primary MDMs and DCs upon Treatment with Pneumococcal MVs

Cytokines released from primary human blood-derived MDMs and DCs were quantified with a cytometric bead array human soluble protein master buffer kit (BD, USA, 558278) and human soluble protein flex set for seven cytokines: interleukin (IL)-1 $\beta$  (BD, 558279), IL-2 (BD, 558270), IL-6 (BD, 558276), IL-8 (BD, 558278), IL-12p70 (BD, 558283), tumor necrosis factor (TNF) (BD, 558273), and interferon- $\gamma$  (IFN- $\gamma$ ) (BD, 558269). The assay was performed per the manufacturer's recommendations. PBS and lipopolysaccharide (LPS)-treated cells ( $250 \text{ ng mL}^{-1}$ ) were prepared as controls. Briefly, standards were prepared by pooling lyophilized standards together and reconstituting them in 4 mL of assay diluent, diluted from 1:2 to 1:256. Fifty microliters of standard dilutions and test samples were mixed gently with an equal volume of mixed capture beads and incubated for 1 h at RT. Next, 50  $\mu\text{L}$  of mixed phycoerythrin (PE) detection reagent was added to the assay tubes and incubated for 2 h at RT. One milliliter of wash buffer was added to each tube and centrifuged at 200 g for 5 min. The supernatant was discarded, and 200  $\mu\text{L}$  of wash buffer was added and vortexed to resuspend the sedimented beads, then measured via flow cytometry (LSR Fortessa, BD Bioscience, USA) after setting the software (BD FACSDiva) as per the supplier's manual. Data were further analyzed using BD FCAP Array software, version 3.0. Cytokine concentrations were determined and compared with the standard calibration curves.

### 3.13. Proteomic Analysis of Pneumococcal MVs

#### 3.13.1. S-Trap Protein Digestion and High-pH Reversed-Phase Peptide Fractionation

sMV and dMV samples containing 20  $\mu\text{g}$  protein were subjected to proteomic analysis. Samples were analyzed before and after purification to account for the influence of SEC purification. Protein concentrations from the samples were determined via BCA assay. S-Trap proteins were digested as per the manufacturer's protocol (www.protifi.com) with minor modifications. Briefly, 2  $\times$  lysis buffer (10% sodium dodecyl sulfate and 100 mM triethylammonium bicarbonate [TEAB], pH 7.55) was added to 20  $\mu\text{g}$  of protein 1:1 (v/v). Afterwards, proteins were reduced in 20 mM dithiothreitol for 10 min at 95  $^{\circ}\text{C}$  and alkylated in 40 mM iodoacetamide for 30 min in the dark. Samples were acidified by adding phosphoric acid to a final concentration of 1.2% (v/v) and diluted 1:7 (v/v) with S-trap binding buffer (90% methanol and 100 mM Tris HCl buffer, pH 7.1). The proteins were digested with 1:50 trypsin in 50 mM TEAB for 3 h at 47  $^{\circ}\text{C}$  in S-Trap microcolumns. The peptides were eluted from the columns using 50 mM TEAB, followed by 0.1% aqueous acetic acid and 60% acetonitrile containing 0.1% acetic acid. The peptides were dried using a vacuum centrifuge, then stored at 20  $^{\circ}\text{C}$  until further processing.

To reduce complexity, samples were fractionated by performing basic reversed-phase peptide fractionation as per the manufacturer's protocol (Pierce high-pH reversed-phase peptide fractionation kit, Thermo Scientific). Briefly, peptides were loaded onto C18 microspin columns (Dr. Maisch ReproSil pur C18, pore size: 300  $\text{\AA}$ , particle size: 5.0  $\mu\text{m}$ ) and eluted with increasing acetonitrile concentrations in eight fractions ranging from 5% to 50% in a high-pH solution (0.1% triethylamine). The eluates of fractions 1 and 5, 2 and 6, 3 and 7, and 4 and 8 were pooled orthogonally. Peptides were dried using a vacuum centrifuge, resuspended in 20  $\mu\text{L}$  of 0.1% acetic acid, and stored at  $-20^{\circ}\text{C}$  until LC-MS/MS measurement.

#### 3.13.2. Mass Spectrometry Data Acquisition and Analysis

Tryptic peptides were separated on an Easy nLC 1200 liquid chromatography system (Thermo Fisher Scientific) with a reversed-phase C18 column (inner diameter: 100  $\mu\text{m}$ , outer diameter: 360  $\mu\text{m}$ , length: 200 mm, in-house packed with Dr. Maisch ReproSil pur C18 120  $\text{\AA}$ , particle size: 3.0  $\mu\text{m}$ ) and a column oven set to 45  $^{\circ}\text{C}$ . Peptides were loaded with 22  $\mu\text{L}$  of buffer A (0.1% acetic acid) at 400 bar and subsequently eluted with a nonlinear 100 min gradient from 1% to 95% of buffer B (acetonitrile with 0.1% acetic acid) at a constant flow rate of 300  $\text{nL min}^{-1}$ . Eluting peptides were analyzed in an Orbitrap Elite mass spectrometer (Thermo Fisher Scientific) in data-dependent mode. The MS1 overview scan was recorded in the orbitrap with a mass window of 300–1700  $m/z$  and a resolution of 60 000. The 20 most intense precursor ions were fragmented; ions with a charge of 1 or unknown were excluded. Fragmentation was performed by collision-induced dissociation, with a collision energy of 35%. The resulting MS/MS spectra were recorded in the linear ion trap.

The .raw files were searched against the UniProt reference proteome of the *S. pneumoniae* strain R6 (ID UP000000586, downloaded on 27 February 2020 with 2030 protein entries and an added CRAP contaminants list) using MaxQuant software (version 1.6.17).<sup>[78]</sup> The search was performed with a maximum of two missed cleavages, oxidation (M) and acetylation (protein N-term) as variable modifications, and carbamidomethylation (C) as a fixed modification. Proteins were considered identified with a minimum of one razor + one unique peptide per protein group. Proteins were quantified label-free using the MaxLFQ algorithm implemented in MaxQuant software. Unique and razor peptides were used for label-free quantification. Resulting data were analyzed with Perseus software (version 1.6.14.0).<sup>[79]</sup> Proteins were considered identified when quantitative values were present in at least 2 of 3 replicates. Label-free quantitation (LFQ) values were log<sub>2</sub> transformed, and two-sided Student's *t*-tests were performed to compare conditions. The mass spectrometry proteomic data were deposited into the ProteomeXchange Consortium via the PRIDE partner repository with the dataset identifier, PXD026462.<sup>[80]</sup>

### 3.14. Statistical Analysis

All data are shown as the means  $\pm$  standard deviation, where the number *n* is independent experiments. All measurements

were performed at least in triplicate in  $n$  independent experiments. Unpaired two-tailed t-tests were performed to compare two groups. Groups of two or more were analyzed using one-way analysis of variance (ANOVA), followed by Tukey's multiple comparison test.

#### 4. Conclusion

Our study revealed that pneumococcal dMVs achieved a higher vesicular yield than did sMVs. dMVs showed a slightly larger particle size range, while both vesicle types exhibited excellent tolerability with several mammalian somatic and immune cell lines. Primary human immune cells showed acceptable compatibility with pneumococcal vesicles. Pneumococcal MVs displayed a gradual uptake into primary MDMs, with a slightly higher trend of uptake values for sMVs than for dMVs. DCs showed comparable uptake for both vesicle types. The vesicles activated both primary MDMs and DCs to release the inflammatory cytokines, TNF and IL-6. Additionally, several strong antigenic proteins and lipoproteins were detected on isolated MVs, confirming their strong potential for protective immunostimulation and as promising vaccine candidates. Although dMVs achieved higher yields, they did not show better cellular uptake or stronger immune responses. More research should be implemented to test the feasibility of dMVs as models for prokaryote membranes.<sup>[81]</sup> In spite of the minimal cytotoxicity observed with primary human immune cells, pneumococcal MVs confer a strong technological advantage being easily produced and more accessible, as well as harboring several strong immunogenic proteins and lipoproteins. This study thus supports applying pneumococcal sMVs as promising vaccine candidates.

#### Supporting Information

Supporting Information is available from the Wiley Online Library or from the author.

#### Acknowledgements

The authors thank Dr. Annette Boese and Dr. Eilien Heinrich for their help with the confocal microscopy imaging, and Petra König and Jana Westhues for their support with the cell cultures and Fawaz Dabbaghie for his help with FASTA files for analysis of proteomic data. The table of contents was created using BioRender.com. Funding: M.M. was supported by an individual Ph.D. fellowship from the German Academic Exchange Service (DAAD) and Egyptian Ministry of Higher Education (GERLS 91664644). G.F. holds a NanoMatFutur grant from the Federal Ministry of Education and Research, Germany (grant number 13XP5029A, BEVA).

Open access funding enabled and organized by Projekt DEAL.

#### Conflict of Interest

The authors declare no conflict of interest.

#### Author Contributions

M.M. performed all M.V. isolation, characterization, and cell testing experiments, analyzed the data and developed the figures. T.K. conducted the

proteomic experiments and analyzed their results. M.K. captured the electron microscopy images. J.H. and A.K.K. provided training, protocols and buffy coats for primary human monocyte isolation and differentiation. D.B. provided support for the proteomic analysis. C.-M.L. helped with the study design and co-supervised the project with G.F. G.F. conceived the overall study and wrote the main manuscript with M.M. All authors reviewed and approved the manuscript.

#### Data Availability Statement

Research data are not shared.

#### Keywords

bacterial membrane vesicles, dendritic cells, extracellular vesicles, pneumococci, primary macrophages, proteomics, vaccines

Received: June 11, 2021

Revised: October 22, 2021

Published online: November 12, 2021

- [1] E. Backhaus, S. Berg, R. Andersson, G. Ockborn, P. Malmström, M. Dahl, S. Nasic, B. Trollfors, *BMC Infect. Dis.* **2016**, *16*, 367.
- [2] *Lancet Infect. Dis.* **2017**, *17*, 1133.
- [3] J. Brown, S. Hammerschmidt, C. Orihuela, *Streptococcus Pneumoniae: Molecular Mechanisms of Host-Pathogen Interactions*, Academic Press, London **2015**.
- [4] WHO, Vol. 2021, World Health Organization, Geneva **2017**.
- [5] E. L. German, C. Solórzano, S. Sunny, F. Dunne, J. F. Gritzfeld, E. Mitsi, E. Nikolaou, A. D. Hyder-Wright, A. M. Collins, S. B. Gordon, D. M. Ferreira, *Vaccine* **2019**, *37*, 3953.
- [6] M. Berman-Rosa, S. O'Donnell, M. Barker, C. Quach, *Pediatrics* **2020**, *145*, e20190377.
- [7] J. N. Weiser, D. M. Ferreira, J. C. Paton, *Nat. Rev. Microbiol.* **2018**, *16*, 355.
- [8] F. Ganaie, J. S. Saad, L. McGee, A. J. van Tonder, S. D. Bentley, S. W. Lo, R. A. Gladstone, P. Turner, J. D. Keenan, R. F. Breiman, M. H. Nahm, *mBio* **2020**, *11*, e00937.
- [9] A. R. Parker, M. A. Park, S. Harding, R. S. Abraham, *Vaccine* **2019**, *37*, 1350.
- [10] M. Kaparakis-Liaskos, R. L. Ferrero, *Nat. Rev. Immunol.* **2015**, *15*, 375.
- [11] M. Mehanny, C. M. Lehr, G. Fuhrmann, *Adv. Drug Deliv. Rev.* **2021**, *173*, 164.
- [12] M. Toyofuku, N. Nomura, L. Eberl, *Nat. Rev. Microbiol.* **2019**, *17*, 13.
- [13] G. P. Dubey, G. B. Malli Mohan, A. Dubrovsky, T. Amen, S. Tsipshtein, A. Rouvinski, A. Rosenberg, D. Kaganovich, E. Sherman, O. Medalia, S. Ben-Yehuda, *Dev. Cell* **2016**, *36*, 453.
- [14] A. Nadeem, J. Oscarsson, S. N. Wai, *Bacterial Membrane Vesicles*, Springer, New York **2020**.
- [15] N. J. Bitto, M. Kaparakis-Liaskos, *Int. J. Mol. Sci.* **2017**, *18*, 1287.
- [16] J. L. Kadurugamuwa, T. J. Beveridge, *J. Bacteriol.* **1995**, *177*, 3998.
- [17] A. J. Manning, M. J. Kuehn, *BMC Microbiol.* **2011**, *11*, 258.
- [18] C. Davies, A. J. Taylor, A. Elmi, J. Winter, J. Liaw, A. D. Grabowska, O. Gundogdu, B. W. Wren, D. J. Kelly, N. Dorrell, *Front. Cell. Infect. Microbiol.* **2019**, *9*, 177.
- [19] M. J. H. Gerritzen, R. H. W. Maas, J. van den Ijssel, L. van Keulen, D. E. Martens, R. H. Wijffels, M. Stork, *Microb. Cell Fact.* **2018**, *17*, 157.
- [20] M. J. H. Gerritzen, D. E. Martens, J. P. Uittenbogaard, R. H. Wijffels, M. Stork, *Sci. Rep.* **2019**, *9*, 4716.
- [21] S. Wang, J. Gao, M. Li, L. Wang, Z. Wang, *Biomaterials* **2018**, *187*, 28.
- [22] L. Jiang, M. Schinkel, M. van Essen, R. M. Schifflers, *Eur. J. Pharm. Biopharm.* **2019**, *145*, 1.

- [23] M. Mehanny, M. Koch, C.-M. Lehr, G. Fuhrmann, *Front. Immunol.* **2020**, *11*, 80.
- [24] L. van der Pol, M. Stork, P. van der Ley, *Biotechnol. J.* **2015**, *10*, 1689.
- [25] J. Frank, M. Richter, C. de Rossi, C. M. Lehr, K. Fuhrmann, G. Fuhrmann, *Sci. Rep.* **2018**, *8*, 12377.
- [26] P. Briaud, R. K. Carroll, *Infect. Immun.* **2020**, 88.
- [27] U. Resch, J. A. Tsatsaronis, A. Le Rhun, G. Stübiger, M. Rohde, S. Kasvandik, S. Holzmeister, P. Tinnefeld, S. N. Wai, E. Charpentier, *mBio* **2016**, *7*, e00207.
- [28] J. Rivera, R. J. Cordero, A. S. Nakouzi, S. Frases, A. Nicola, A. Casadevall, *Proc. Natl. Acad. Sci. U S A* **2010**, *107*, 19002.
- [29] C. Coelho, L. Brown, M. Maryam, R. Vij, D. F. Q. Smith, M. C. Burnet, J. E. Kyle, H. M. Heyman, J. Ramirez, R. Prados-Rosales, G. Lauvau, E. S. Nakayasu, N. R. Brady, A. Hamacher-Brady, I. Coppens, A. Casadevall, *J. Biol. Chem.* **2019**, *294*, 1202.
- [30] M. Toyofuku, G. Carcamo-Oyarce, T. Yamamoto, F. Eisenstein, C. C. Hsiao, M. Kurosawa, K. Gademann, M. Pilhofer, N. Nomura, L. Eberl, *Nat. Commun.* **2017**, *8*, 481.
- [31] A. Olaya-Abril, R. Prados-Rosales, M. J. McConnell, R. Martín-Peña, J. A. González-Reyes, I. Jiménez-Munguía, L. Gómez-Gascón, J. Fernández, J. L. Luque-García, C. García-Lidón, H. Estévez, J. Pachón, I. Obando, A. Casadevall, L. A. Pirofski, M. J. Rodríguez-Ortega, *J. Proteomics* **2014**, *106*, 46.
- [32] P. Drücker, I. Iacovache, S. Bachler, B. Zuber, E. B. Babiychuk, P. S. Dittrich, A. Draeger, *Biomater. Sci.* **2019**, *7*, 3693.
- [33] B. Armistead, P. Quach, J. M. Snyder, V. Santana-Ufret, A. Furuta, A. Brokaw, L. Rajagopal, *J. Infect. Dis.* **2021**, *223*, 1488.
- [34] M. V. Surve, A. Anil, K. G. Kamath, S. Bhutda, L. K. Sthanam, A. Pradhan, R. Srivastava, B. Basu, S. Dutta, S. Sen, D. Modi, A. Banerjee, *PLoS Pathog.* **2016**, *12*, e1005816.
- [35] T. Kuhn, M. Koch, G. Fuhrmann, *Small* **2020**, *16*, 2003158.
- [36] C. W. Choi, E. C. Park, S. H. Yun, S. Y. Lee, S. I. Kim, G. H. Kim, *J. Immunol. Res.* **2017**, *2017*, 7931982.
- [37] M. Codemo, S. Muschiol, F. Iovino, P. Nannapaneni, L. Plant, S. N. Wai, B. Henriques-Normark, *mBio* **2018**, *9*, e00559.
- [38] K. Schepers, F. Mouchet, V. Dirix, I. De Schutter, K. Jotzo, V. Verscheure, P. Geurts, M. Singh, J. P. Van Vooren, F. Mascart, *Clin. Vaccine Immunol.* **2014**, *21*, 111.
- [39] T. Tanaka, M. Narazaki, K. Masuda, T. Kishimoto, *Adv. Exp. Med. Biol.* **2016**, *941*, 79.
- [40] A. K. Mehta, D. T. Gracias, M. Croft, *Cytokine* **2018**, *101*, 14.
- [41] P. Stinccone, K. N. Miyamoto, P. P. R. Timbe, I. Lieske, A. Brandelli, *J. Proteomics* **2020**, *226*, 103906.
- [42] N. Y. Yu, J. R. Wagner, M. R. Laird, G. Melli, S. Rey, R. Lo, P. Dao, S. C. Sahinalp, M. Ester, L. J. Foster, F. S. Brinkman, *Bioinformatics* **2010**, *26*, 1608.
- [43] C. S. Yu, Y. C. Chen, C. H. Lu, J. K. Hwang, *Proteins* **2006**, *64*, 643.
- [44] S. Kohler, F. Voß, A. Gómez Mejía, J. S. Brown, S. Hammerschmidt, *FEBS Lett.* **2016**, *590*, 3820.
- [45] A. Kovacs-Simon, R. W. Titball, S. L. Michell, *Infect. Immun.* **2011**, *79*, 548.
- [46] G. Mao, Y. Zhao, X. Kang, Z. Li, Y. Zhang, X. Wang, F. Sun, K. Sankaran, X. C. Zhang, *Nat. Commun.* **2016**, *7*, 10198.
- [47] S. Chimalapati, J. M. Cohen, E. Camberlein, N. MacDonald, C. Durmort, T. Vernet, P. W. Hermans, T. Mitchell, J. S. Brown, *PLoS One* **2012**, *7*, e41393.
- [48] G. Rajam, J. M. Anderton, G. M. Carlone, J. S. Sampson, E. W. Ades, *Crit. Rev. Microbiol.* **2008**, *34*, 131.
- [49] A. R. Kerr, P. V. Adrian, S. Estevão, R. de Groot, G. Alloing, J. P. Claverys, T. J. Mitchell, P. W. Hermans, *Infect. Immun.* **2004**, *72*, 3902.
- [50] J. Zahlten, Y. J. Kim, J. M. Doehn, T. Pribyl, A. C. Hocke, P. García, S. Hammerschmidt, N. Suttrop, S. Hippenstiel, R. H. Hübner, *J. Infect. Dis.* **2015**, *211*, 1822.
- [51] T. Herta, A. Bhattacharyya, C. Bollensdorf, C. Kabus, P. García, N. Suttrop, S. Hippenstiel, J. Zahlten, *Sci. Rep.* **2018**, *8*, 5723.
- [52] K. Jahn, S. Handtke, R. Palankar, S. Weißmüller, G. Nouailles, T. P. Kohler, J. Wesche, M. Rohde, C. Heinz, A. F. Aschenbrenner, M. Wolff, J. Schüttrumpf, M. Witzentrath, S. Hammerschmidt, A. Greinacher, *Blood Adv.* **2020**, *4*, 6315.
- [53] K. Subramanian, D. R. Neill, H. A. Malak, L. Spelmink, S. Khandaker, G. Dalla Libera Marchiori, E. Dearing, A. Kirby, M. Yang, A. Achour, J. Nilvebrant, P. Nygren, L. Plant, A. Kadioglu, B. Henriques-Normark, *Nat. Microbiol.* **2019**, *4*, 62.
- [54] A. T. Nishimoto, J. W. Rosch, E. I. Tuomanen, *Front. Microbiol.* **2020**, *11*, 1543.
- [55] A. Thanawastien, K. E. Joyce, R. T. Cartee, L. A. Haines, S. I. Pelton, R. K. Tweten, K. P. Killeen, *Vaccine* **2021**, *39*, 1652.
- [56] M. L. Ferrando, S. Fuentes, A. de Greeff, H. Smith, J. M. Wells, *Microbiology* **2010**, *156*, 2818.
- [57] G. Bethe, R. Nau, A. Wellmer, R. Hakenbeck, R. R. Reinert, H. P. Heinz, G. Zysk, *FEMS Microbiol. Lett.* **2001**, *205*, 99.
- [58] M. Q. Ali, T. P. Kohler, G. Burchhardt, A. Wüst, N. Henck, R. Bolsmann, F. Voß, S. Hammerschmidt, *Front. Cell. Infect. Microbiol.* **2020**, *10*, 613467.
- [59] M. Seiberling, M. Bologa, R. Brookes, M. Ochs, K. Go, D. Neveu, T. Kamtchoua, P. Lashley, T. Yuan, S. Gurunathan, *Vaccine* **2012**, *30*, 7455.
- [60] M. Bologa, T. Kamtchoua, R. Hopfer, X. Sheng, B. Hicks, G. Bixler, V. Hou, V. Pehlic, T. Yuan, S. Gurunathan, *Vaccine* **2012**, *30*, 7461.
- [61] M. M. Ochs, K. Williams, A. Sheung, P. Lheritier, L. Visan, N. Rouleau, E. Proust, A. de Montfort, M. Tang, K. Mari, R. Hopfer, S. Gallichan, R. H. Brookes, *Hum. Vaccines Immunother.* **2016**, *12*, 2946.
- [62] M. L. Oliveira, E. N. Miyaji, D. M. Ferreira, A. T. Moreno, P. C. Ferreira, F. A. Lima, F. L. Santos, M. A. Sakauchi, C. S. Takata, H. G. Higashi, I. Raw, F. S. Kubrusly, P. L. Ho, *PLoS One* **2010**, *5*, e10863.
- [63] Y. C. Kye, S. M. Park, B. S. Shim, J. Firdous, G. Kim, H. W. Kim, Y. J. Ju, C. G. Kim, C. S. Cho, D. W. Kim, J. H. Cho, M. K. Song, S. H. Han, C. H. Yun, *Acta Biomater.* **2019**, *90*, 362.
- [64] B. Li, X. Chen, J. Yu, Y. Zhang, Z. Mo, T. Gu, W. Kong, Y. Wu, *Microb. Pathog.* **2018**, *123*, 115.
- [65] D. Wang, J. Lu, J. Yu, H. Hou, K. Leenhouts, M. L. Van Roosmalen, T. Gu, C. Jiang, W. Kong, Y. Wu, *Immunol. Invest.* **2018**, *47*, 403.
- [66] D. Mistry, R. A. Stockley, *Int. J. Biochem. Cell Biol.* **2006**, *38*, 1244.
- [67] Z. Wang, J. Rahkola, J. S. Redzic, Y. C. Chi, N. Tran, T. Holyoak, H. Zheng, E. Janoff, E. Eisenmesser, *Nat. Commun.* **2020**, *11*, 6063.
- [68] O. Kotelnikova, A. Alliluev, A. Zinchenko, L. Zhigis, Y. Prokopenko, E. Nokel, O. Razgulyaeva, V. Zueva, M. Tokarskaya, N. Yastrebova, E. Gordeeva, T. Melikhova, E. Kaliberda, L. Rumsh, *Microbes Infect.* **2019**, *21*, 336.
- [69] C. Murdoch, R. C. Read, Q. Zhang, A. Finn, *J. Infect. Dis.* **2002**, *186*, 1253.
- [70] B. Maestro, J. M. Sanz, *Antibiotics* **2016**, *5*, 21.
- [71] N. R. Scott, B. Mann, E. I. Tuomanen, C. J. Orihuela, *Vaccines* **2021**, *9*, 209.
- [72] W. Y. Chan, C. Entwisle, G. Ercoli, E. Ramos-Sevillano, A. McIlgorm, P. Cecchini, C. Bailey, O. Lam, G. Whiting, N. Green, D. Goldblatt, J. X. Wheeler, J. S. Brown, *Infect. Immun.* **2019**, 87.
- [73] E. Schulz, A. Karagianni, M. Koch, G. Fuhrmann, *Eur. J. Pharm. Biopharm.* **2020**, *146*, 55.
- [74] E. Schulz, A. Goes, R. Garcia, F. Panter, M. Koch, R. Muller, K. Fuhrmann, G. Fuhrmann, *J. Control Released* **2018**, *290*, 46.
- [75] A. Dembek, S. Laggai, S. M. Kessler, B. Czepukojc, Y. Simon, A. K. Kierner, J. Hoppstädter, *Immunobiology* **2017**, *222*, 786.
- [76] J. Hoppstädter, M. Seif, A. Dembek, C. Cavellius, H. Huwer, A. Kraegeloh, A. K. Kierner, *Front. Pharmacol.* **2015**, *6*, 55.
- [77] F. Geissmann, C. Prost, J. P. Monnet, M. Dy, N. Brousse, O. Hermine, *J. Exp. Med.* **1998**, *187*, 961.

- [78] S. Tyanova, T. Temu, J. Cox, *Nat. Protoc.* **2016**, *11*, 2301.
- [79] S. Tyanova, T. Temu, P. Sinitcyn, A. Carlson, M. Y. Hein, T. Geiger, M. Mann, J. Cox, *Nat. Methods* **2016**, *13*, 731.
- [80] Y. Perez-Riverol, A. Csordas, J. Bai, M. Bernal-Llinares, S. Hewapathirana, D. J. Kundu, A. Inuganti, J. Griss, G. Mayer, M. Eisenacher, E. Pérez, J. Uszkoreit, J. Pfeuffer, T. Sachsenberg, S. Yilmaz, S. Tiwary, J. Cox, E. Audain, M. Walzer, A. F. Jarnuczak, T. Ternent, A. Brazma, J. A. Vizcaíno, *Nucleic Acids Res.* **2019**, *47*, D442.
- [81] R. Richter, C. M. Lehr, *Adv. Drug Deliv. Rev.* **2021**, *173*, 492.